Neutron and proton dynamics of ^{48}Ca levels and γ-ray decays from neutron inelastic scattering

J. R. Vanhoy* and M. T. McEllistrem
Department of Physics and Astronomy, University of Kentucky, Lexington, Kentucky 40506

Sally F. Hicks
Department of Physics, University of Dallas, Irving, Texas 75062

R. A. Gatenby, E. M. Baum, E. L. Johnson, G. Molnár,† and S. W. Yates
Department of Chemistry, University of Kentucky, Lexington, Kentucky 40506
(Received 16 April 1991)

Differential cross sections were measured for the ^{48}Ca$(n, n'\gamma)$ reactions at incident energies between 4.8 and 8.0 MeV. Excitation energies, spins, level lifetimes, γ-ray branching ratios, and γ-ray production cross sections were determined. Members of the doublet at 4.50 MeV are clearly identified and assigned spins of 4^+ and 3^-. Inelastic neutron scattering cross sections were inferred from the γ-ray branching ratios and production cross sections. The inferred cross sections are in excellent agreement with those measured in a separate neutron detection experiment, and with a recent vibrational model coupled-channels analysis of the ^{48}Ca(n, n') data. Comparison of level excitations produced by neutrons and other hadrons with electromagnetic strengths shows very different mixtures of neutron and proton particle-hole amplitudes for different levels.

PACS number(s): 23.20.Lv, 21.10.Tg, 25.40.Fq, 27.40.+z

I. INTRODUCTION

The doubly magic nucleus ^{48}Ca provides a very stable core for nearby nuclei. Evidence for its stability is found in the low-lying level scheme [1, 2] of ^{49}Ca, which is just that of a single neutron coupled to the ground state of ^{48}Ca. Additional evidence for the stability of that core comes from other nuclei; for example, ^{51}V presents a beautiful illustration of a three $f_{7/2}$ proton spectrum [3]. Random phase approximation (RPA) calculations [4] presented further support for the stability of the ^{48}Ca core, since pairing correlations were shown to play a small role in the ground state. This stability is important, since it enables us to treat scattering from ^{48}Ca as that of neutrons coupled to $A = 48$ core excitations, with just a few excitations included for neutron energies of several MeV. Core excitations, in fact, should become important only at high excitation energies in ^{49}Ca.

Low energy neutron scattering from ^{48}Ca shows strong, simple intermediate structure resonances [5, 6] which correspond to ^{49}Ca single-particle states coupled to 3^- core excitations. A strong coupling analysis [6] of the differential scattering cross sections measured at the University of Kentucky [6] and total cross sections measured at Oak Ridge National Laboratory (ORNL) [5] described this intermediate resonance structure. The model rests on the fact that the low-lying levels of ^{49}Ca are indeed good single nucleon excitations [1, 2]; the model's success helps to confirm the importance of single particle amplitudes of ^{49}Ca levels.

The neutron scattering study also fixed electric octupole coupling strengths for inelastic scattering to the first two 3^- levels in ^{48}Ca. The resulting strengths indicate that the two 3^- excitations share the strength of the single octupole excitation in ^{40}Ca. This leads to the suggestion that the extra filled neutron shell in ^{48}Ca splits the 3^- core into two fragments, roughly dominated by proton and neutron excitations separately. This scattering interpretation [6] rested in part, however, on describing inelastic scattering cross sections to levels in ^{48}Ca which could not be resolved in the neutron detection experiment [6].

Thus there is strong incentive to learn as much as possible about the excitations of ^{48}Ca, and to separate inelastic neutron scattering cross sections to levels too closely spaced to be resolved in neutron detection. The spins and parities of levels, lifetimes and transition rates, and inelastic neutron scattering cross sections to well-resolved levels are fixed in this $(n, n'\gamma)$ study, in conjunction with the earlier neutron detection experiment [6]. The present experiment complements the earlier one by exploiting the high energy resolution available with current γ-ray detectors. The results of this study include three newly discovered levels, and nine unique spin assignments. The descriptions of most excited levels and their decays up to

*Present address: Physics Department, U.S. Naval Academy, Annapolis, MD 21402.
†On leave from the Institute of Isotopes, H-1525 Budapest, Hungary.

an excitation energy of 7.5 MeV are included; the decay lifetimes are determined for several levels.

A great deal of prior work has been done on charged hadron and electron scattering to core collective excitations of ^{48}Ca, but prior neutron scattering information is sparse. The present neutron scattering experiment and that of Ref. [6] offer the first opportunity to compare neutron, electromagnetic, and other hadron excitation strengths, and thus separate the roles of neutron and proton particle-hole excitations for collective levels.

II. EXPERIMENTAL PROCEDURES

Excitation functions and angular distributions for inelastic neutron scattering (INS) were measured with the pulsed neutron scattering facility at the 7 MV Van de Graaff accelerator of the University of Kentucky. A 2 MHz pulsed deuteron beam was utilized to produce neutrons via the ^{2}H$(d,n)^3$He reaction. Samples were made by compressing 4.5 g of 96% enriched ^{48}Ca (in carbonate form) into a slab of dimensions 2.7×2.7×0.8 cm [7]. The slab was enclosed in a delrin box of thickness ~ 4 mils and centered in front of the gas cell at an angle of 45° with respect to the beam axis and at a distance of ~ 5 cm from the center of the deuterium gas cell. Neutron flux was monitored using a long counter placed at 50° with respect to the beam. Excitation functions were corrected for variations of the angular dependence of the ^{2}H$(d,n)^3$He source reaction with incident deuteron energy.

Deexcitation gamma rays were detected with a 20% efficient intrinsic Ge detector. Time-of-flight techniques were used to discriminate between the prompt γ rays and neutron induced background events. A typical detector spectrum is shown in Fig. 1. The γ-ray background lines were identified by the use of carbon and water samples, which scatter neutrons toward the detector, but produce only a few well known transitions. Yields and positions of the peaks of interest were extracted using the multiparameter line-shape fitting code HYPERMET [8]. Yields were corrected for incident neutron attenuation and multiple scattering, exit γ-ray absorption, and Ge detector efficiency. Because of the small sample size, the corrections are small (incident neutron attenuation ~1–2%, neutron multiple scattering ~ 1%, γ-ray absorption ~ 2–5%). The detector's energy response and relative detection efficiency were calibrated with ^{56}Co and ^{152}Eu radioactive sources. These sources provide very well known γ-ray energies and relative intensities [9]. The resolution of the detection system as determined with these sources was 2.0 keV FWHM at 1.3 MeV and 3.1 keV FWHM at 3.2 MeV.

The detector's energy spectra were calibrated in three energy regions. Transition energies less than ~ 3.2 MeV can be accurately determined using ^{56}Co and ^{152}Eu sources. Most of the γ-ray transitions of interest in this experiment lie in the 600–1600 keV range; the ^{56}Co lines from 846.8 to 2015 keV were most appropriate to calibrate that region. The uncertainty of transition energies determined in this region is ~ 0.1 keV. There are several high energy transitions whose energies lie significantly above the range of our calibration sources. For the transitions between 2500 and 5320 keV we use a procedure similar to that of Tape *et al.* [10]—the ^{48}Ca lines at 3832.2 and 4507.3 keV have strong full-energy and escape peaks. The separation of the full-energy and escape peaks was used to determine the slope of the linear calibration and the intercept was then fixed using the 3547.93-keV ^{56}Co line. The energy uncertainty is ~ ± 0.5 keV in this region. The third group of transitions lies between 6300 and 8000 keV. Calibration in the highest energy region was performed using the ^{16}O background lines [9] from the sample at 6130.43(5), 6918.8(6), and 7116.85(14) keV. The energy uncertainty is ~ ± 1 keV in this region. Most high-lying excited levels decay by cascades through the first excited level. Thus, although all low energy transitions are fixed with good accuracy, the actual excitation energies of states are uncertain by ~ ± 0.5 keV.

Excitation functions, or γ-ray yields as a function of incident neutron energy, were measured at a detection angle of 90° and over the incident neutron energy range from 4.8 to nearly 8 MeV. The γ-ray yield thresh-

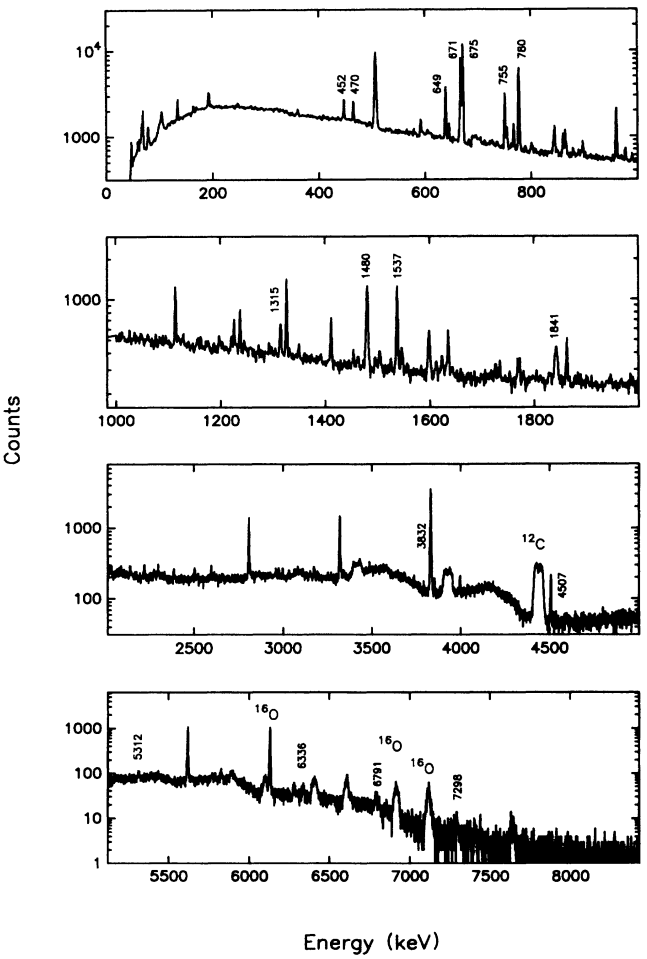

FIG. 1. Gamma-ray spectrum taken at an incident neutron energy of 8.0 MeV. Lines from ^{48}Ca, ^{12}C, and ^{16}O, present in the target material, appear in the spectrum.

olds found in these energy-dependent yields were important for placing transitions in the decay scheme of ^{48}Ca. Gamma-ray angular distributions were measured at incident neutron energies of E_n = 4.8, 6.2, and 8.0 MeV for as many as nine detector angles. Data were analyzed to extract branching ratios, γ-ray production cross sections, and spin assignments. Angular distributions were fitted by an even-order Legendre polynomial expansion. The usual procedure for making a spin assignment to a level is to postulate an assignment consistent with the various decays of that level, and then test with calculated angular distributions for all possible multipole mixtures of the γ-ray decay. One tests whether the measured angular distribution could be consistent with the postulated spin assignment and any ratio of multipole amplitudes in the decay. The ratio of multipole amplitudes in the decay transition is defined as $\delta =< |L+1| > / < |L| >$ where $< |L| >$ is defined as the reduced transition amplitude for multipole order L. The phase convention of δ and the reduced transition amplitudes follow the definitions of Rose and Brink [11]. The actual calculations of angular distributions are generated with the compound nucleus code CINDY [12] using the optical model parameters of Hicks [7]. Spin assignments were determined with standard χ^2 versus δ plots such as shown in Fig. 2. The most confident spin assignments are obtained from the E_n = 4.8 and 6.2 MeV data, since confusion caused by cascade feeding of levels is least at these lower incident energies.

Gamma-ray production cross sections were derived from the Legendre polynomial fits. The INS cross section to an individual level can be inferred from the difference of the cross sections of transitions depopulating the level and those γ-ray transitions feeding the level. Cross-section calibration was performed for incident energies above 5 MeV using results from several evaluations of the γ-ray production cross sections [13, 14] for neutron scattering to the first excited state of ^{12}C. The several evaluations provide results in good agreement with each other. The ^{12}C$(n, n'\gamma)$ yields were available as an internal calibration due to the presence of carbon in our $CaCO_3$ scattering sample. Relative cross section uncertainties affecting reproducibility are typically a few percent, and determined primarily by counting statistics. The systematic uncertainties in cross sections are dominated by the uncertainties in the ^{12}C$(n, n'\gamma)$ cross sections [14]. The systematic uncertainties are $\sim \pm$ 8%. The smallest observable γ-ray peaks were those corresponding to production cross sections of $\sim$ 3 mb (for $E_\gamma \sim$ 2 MeV).

Lifetimes were extracted with the Doppler shift attenuation method (DSAM). The measured energy of a gamma ray as function of detection angle is $E_\gamma(\theta) = E_{\gamma_0}[1 + F(\tau)\beta \cos\theta]$, where β is the initial velocity of the recoiling nucleus (relative to the speed of light), E_{γ_0} is the true transition energy, and $F(\tau)$ is the attenuation factor which carries the dependence on the mean lifetime. All lifetimes discussed in this work are mean lives. Typical recoil velocities in the present experiment are $\beta \sim$ 0.002. Lifetime measurements with the DSAM require a very precise ($\ll$ 1 keV) knowledge of the transition energies. To assure the maximum possible accuracy, data were taken using a ^{56}Co radioactive source as an internal energy calibration in each spectrum.

Attenuation factors were extracted using a least-squares fit of peak energy centroids versus cosθ. The formalism of Blaugrund [15] is used to relate the measured attenuation factors to lifetimes (τ). The calculation requires a knowledge of the stopping power of the recoil nucleus in the target material. The stopping power is composed of two contributions: energy loss in the electron cloud and hard collisions with the atomic nuclei.

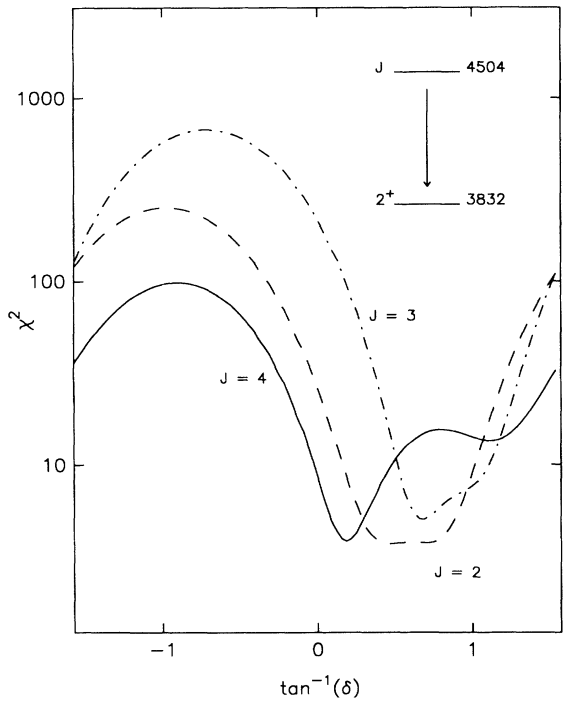

FIG. 2. χ^2 fits to the 671 keV, 4503.6 → 3832.2-keV transition at E_n = 4.8 MeV. The J = 4 assignment is the only acceptable solution if transitions to this state from levels of highly known spin and parity are also considered.

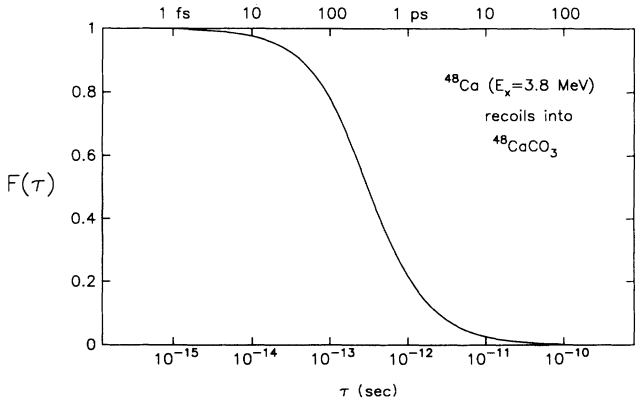

FIG. 3. Dependence of the Doppler shift attenuation factor on level lifetime for the 3832-keV first excited state. States with lifetimes in the range $\sim$ 10 fs to $\sim$ 5 ps can be determined in the present experiment.

TABLE I. ^{48}Ca γ rays observed from the $(n, n'\gamma)$ reaction at 4.8 MeV.

E_γ (keV)	Legendre coefficients a_2	a_4	Placement $E_i \rightarrow E_f$
451.6	-0.063(72)		4283.7-3832.2
671.4	0.66(07)		4503.6-3832.2
675.1	-0.41(05)		4507.3-3832.2
780.1	-0.49(11)		4612.3-3832.2
3832.2	0.36(3)		3832.2-g.s.
4507.3	1.06(31)	0.90(34)	4507.3-g.s.

Empirical expressions for these stopping powers are those of Engelbertink [16]. The relationship between attenuation factors and lifetimes for the 3832.2-keV transition is shown in Fig. 3. Only states with lifetimes of $\sim$ 10 fs to $\sim$ 5 ps can be accurately determined in the present experiment, unless the lines are exceptionally strong. Feeding from higher-lying levels can have disastrous effects on lifetime determination, unless accurate corrections can be made.

III. RESULTS FOR INDIVIDUAL LEVELS

Experimental results include the discovery of three new levels and the clarification of the energy placements of two others. New levels are identified through newly observed transitions. Spin and some parity assignments have been made, or definitely confirmed, for nine levels, and mean lifetimes have been measured for five levels. This information, combined with that previously known, gives us a basis for characterizing excited levels up to nearly 7.5-MeV excitation energy. Legendre coefficients from the angular distribution data measured at 4.8-MeV neutron energy are given in Table I. Results of the analysis of the 6.2-MeV data are summarized in Tables II and III, and that of the 8.0-MeV data in Tables IV and V.

The discussion of levels is presented here only for those levels for which the present work provides substantial new information. Thus the listing of levels is incomplete above 5.5-MeV excitation energy. Since we have a dynamic sensitivity range represented by cross sections ≥ 3 mb, we would expect to see all levels except those for which the spin $J > 6$.

3832.2-keV level. The first excited state has been well studied and is known to have spin and parity 2^+. Its lifetime was previously determined to be 53 $\pm$ 24 fs using a $(p, p'\gamma)$ DSAM coincidence measurement at $E_p = 7.60$ MeV [17]. In the present experiment, Doppler broadening and shifts of the line were observed at $E_n = 5.1$, 6.2, and 8.0 MeV. Close inspection of the line shape at $E_n = 6.2$ MeV as a function of angle, as shown in Fig. 4, reveals the presence of distinct shifted and unshifted components. The first excited state is strongly fed from the higher-lying, long-lived states, and this feeding generates an unshifted contribution to the line shape. A fit to the 3832.2-keV transition was therefore attempted as

TABLE II. ^{48}Ca γ rays observed from the $(n, n'\gamma)$ reaction at 6.2 MeV.

E_γ (keV)	Legendre coefficients a_2	a_4	Placement $E_i \rightarrow E_f$
451.6	-0.04(04)		4283.7-3832.2
468.7	0.32(18)	0.46(21)	5729.6-5260.9
642.7	-0.21(04)		5146.3-4503.6
648.4	-0.14(16)		5260.9-4612.3
671.4	0.23(02)	-0.08(03)	4503.6-3832.2
675.1	-0.29(02)		4507.3-3832.2
753.8	-0.40(07)		5260.9-4507.3
757.5	0.28(20)		5370.0-4612.3
780.1	-0.27(03)		4612.3-3832.2
803.9	0.04(30)		5312.3-4507.3
862.7	0.15(14)		5370.0-4507.3
866.9	-0.25(12)	-0.30(15)	5370.0-4503.6
1226.	0.56(17)		5729.6-4503.6
1480.2	0.36(02)		5312.3-3832.2
1537.8	-0.41(05)	-0.14(07)	5370.0-3832.2
3832.2(5)	0.16(02)	-0.09(04)	3832.2-g.s.
shifted[a]	0.33 (06)	-0.21(11)	
4507.3(5)	0.62(06)	0.33(08)	4507.3-g.s.
5312.3(5)	0.37(07)	-0.36(12)	5312.3-g.s.

[a] Doppler shifted component of ground-state transition.

two distinct peaks, one a shifted and broadened peak arising from direct neutron excitation of the level and the other a sharp, unshifted component arising from cascades from higher energy, long-lived states. A further complication associated with this separation was noted at $E_n = 6.2$ MeV because there is an additional small cascade contribution from a level with an intermediate lifetime. This level lies at 5312.3 keV with a lifetime of 335 fs; close examination of the 3832.2-keV line revealed a third, shifted component corresponding to the 335 fs cascade also present. Fortunately the DSAM measurement could be done still lower in energy, at $E_n = 5.1$ MeV where there is no feeding from the 5312.3-keV level and thus no distortion from this third component. The attenuation factor determined from the 5.1-MeV data is well fixed at $F(\tau) = 0.84 \pm 0.03$, corresponding to a lifetime of $\tau = 60\ ^{-12}_{+11}$ fs. This is in excellent accord with the 59 fs reported in the compilation of Raman *et al.* [18]. The 2^+_1 ground-state transition strength, $B(E2) = 1.6 \pm 0.4$ Weisskopf units (W.u.), agrees well with the $B(E2)$ determined [19] from electron scattering, $B(E2) = 1.7 \pm 0.2$ W.u. and certainly also with that measured in proton inelastic scattering [17,20], $B(E2) = 1.7 \pm 0.8$ W.u. There is a very marked difference, however, with the inelastic alpha scattering results [21], $B(E2) = 4.9 \pm 0.8$ W.u.

Because of the peculiar line shape of the 3832.2-keV transition, we are also able to obtain directly the INS cross section to this level. Essentially all the contribution to the production cross section from cascade feeding appears in the unshifted component; the cascade from the 5312.3-keV level is quite small, less than 10% of the yield from inelastic scattering to the level. A fit to the angular distribution of the shifted component at $E_n = 6.2$ MeV gives a Legendre expansion of the form

$$W(\theta) = 1 + a_2 P_2(\cos(\theta)) + a_4 P_4(\cos(\theta))$$

with coefficients of $a_2 = 0.33 \pm 0.06$ and $a_4 = -0.21 \pm 0.11$—in good agreement with the strongly aligned values for a $2^+ \rightarrow 0^+$ transition. The INS cross section obtained from the shifted component is 254 ± 21 mb—in excellent agreement with the result determined by the standard method of subtracting feeding contributions, as presented in Table III. At $E_n = 8.0$ MeV the agreement between methods of determining the INS cross section is not expected to be quite so good, due to the accumulation of uncertainties when subtracting the larger number of feeding contributions.

4283.7-keV level. The level at 4283.7 keV is known to have spin and parity 0^+. This state decays to the first excited state by γ-ray emission and to the ground state by conversion electrons. The isotropy of the 4283.7 $\rightarrow$ 3832.2-keV transition is noted because it helps to warrant that the angular distributions are well measured in spite of the very small scattering sample.

4503.6-keV level. The existence of a 4503.6-keV level near the 4507.3-keV level was first suggested in the β-decay experiments of Multhauf [22]. Further evidence for this state is seen in the $(p,p'\gamma)$ coincidence experiments [23] of Tape *et al.* The state was assigned spin 4 primarily on the basis of shell model calculations which predict a 4^+ state in the region $E_x = 3.8-5.0$ MeV. Clear

TABLE III. Levels and cross sections from $E_n = 6.2$ MeV data.

E_x[a] (keV)	J^π	E_γ (keV)	E_f (keV)	Production cross section[b] (mb)	INS cross section (mb)	
3832.2	2+	3832.2	g.s.	1113.0(2.0)	241.9(6.1)	(254 ± 21)[c]
4283.7	0+	451.6	3832.2	56.7(0.6)	56.7(0.6)	
4503.6	4+	671.4	3832.2	289.1(4.0)	217.9(4.3)	
4507.3	3-	4507.3	g.s.	53.0(2.5)	202.8(3.8)	
		675.1	3832.2	224.4(2.6)		
4612.3	3(+)	780.1	3832.2	156.0(2.3)	128.2(2.3)	
5146.2	5+	642.7	4503.6	52.0(0.7)	52.0(0.7)	
5260.9	4(-)	753.8	4507.3	54.9(0.9)	52.9(1.0)	
		648.4	4612.3	11.9(0.2)		
5312.3	2+	5312.2	g.s.	15.4(0.4)	120.7(2.2)	
		1480.2	3832.2	99.2(2.1)		
		803.9	4507.3	6.1(0.3)		
5370.0	3-	1537.8	3832.2	45.7(0.8)	94.4(1.7)	
		866.9	4503.6	19.2(1.3)		
		862.7	4507.3	13.6(0.5)		
		757.5	4612.3	15.9(0.4)		
5729.6	5-	468.7	5260.9	13.9(0.5)	13.9(0.5)	
		1226.	4503.6	0.0		
				Total INS	1179.1 $\pm$ 6.9 mb	

[a] Uncertainties in level energies are $\approx \pm 0.5$ keV.

[b] Uncertainties tabulated are from counting statistics and Legendre polynomial fits only. An additional systematic uncertainty of approximately 8% arises primarily from uncertainties in the ^{12}C calibration cross sections.

[c] Value from the Doppler-shifted component of the 3832.2-keV line.

separation of members of the 4503.6/4507.3 keV doublet has been made for the first time in the present experiment. The deexcitation gamma rays from each member of the doublet to the 3832.2-keV 2^+ state are clearly identified in Fig. 5. The angular distribution of the 4503.6 → 3832.2-keV line is characteristic of a stretched $E2$ transition, although not unique to a spin 4^+ assignment—several mixed $M1/E2$ transitions from levels with spins 2, 3, and 4 would yield the same anisotropies. This is indicated in the χ^2 versus δ plot of Fig. 2. However, one may use the cascades from higher-lying levels with reasonably well determined spins to restrict the spin assignment. In particular, the angular distribution of the decay of the 5146.2-keV 5^+ state has $a_2 = -0.21 \pm 0.04$, implying an $L = 1$ decay to the 4503.6-keV level. Thus a spin assignment of $J^\pi = 4^+$ is definitely confirmed for the 4503.6-keV level. The lifetime is too long to be measured in the present experiment.

TABLE IV. ^{48}Ca γ rays observed from the $(n, n'\gamma)$ reaction at 8.0 MeV.

E_γ[a] (keV)	Legendre coefficients a_2	a_4	Placement $E_i \rightarrow E_f$
451.6	0.04(05)		4283.7-3832.2
468.7	-0.25(14)		5729.6-5260.9
642.7	-0.17(06)		5146.2-4503.6
648.4	-0.38(19)		5260.9-4612.3
671.4	0.31(07)		4503.6-3832.2
675.1	-0.21(05)		4507.3-3832.2
753.8	-0.36(11)		5260.9-4507.3
757.5	0.19(10)		5370.0-4612.3
780.1	-0.26(05)		4612.3 -3832.2
803.9	0.22(45)		5312.3-4507.3
862.7	-0.03(19)	-0.19 (23)	5370.0-4507.3
866.9	-0.23(16)	-0.21 (18)	5370.0-4503.6
1199.3	0.02(34)		6345-5146.2
1226	0.09(17)		5729.6-4503.6
1315.8	0.07(26)		6686-5370.0
1480.2	0.11(07)		5312.3-3832.2
1504.0	0.05(23)		6649-5146.2
1525.7	-0.43(53)		6896-5370.0
1537.8	-0.31(13)		5370.0-3832.2
1597.8	-0.37(07)		6105.3-4507.3
1733.5	-0.26(24)		6345-4612.3
1767.8	-1.18(38)	-0.86 (48)	7498-5729.6
1841.2	0.11(10)		6345-4503.6
2036.8	-0.79(22)		6649-4612.3
2073.9	0.83(1.22)		6686-4612.3
2145.1	-0.52(14)	-0.90 (23)	6649-4503.6
2273.1	-1.02(63)		6105.3-3832.2
2301.9	0.37(29)		6807-4503.6
2389.0	-0.13(30)		6896-4507.3
2524.9	-0.45(25)		7032-4503.6
2974.8	-1.01(36)		6807-3832.2
2998.7	0.23(47)		6830-3832.2
3175.5	-0.28(23)		7008-3832.2
3483.9	0.44(23)		7298-3832.2
3736.6	0.22(42)		7569-3832.2
3832.2	0.29(04)		3832.2-g.s.
shifted[b]	0.60(09)		
4507.3	0.39(09)		4507.3-g.s.
5312.2			5312.3-g.s.
6336.4	0.28(18)		6336.4-g.s.
6791.0	-0.70(20)		6791-g.s.
7298	0.81(37)		7298-g.s.
7370			7370-g.s.
7440	1.74(51)		7440-g.s.

[a] Uncertainties in the γ-ray transition energies are approximately ± 0.1 keV for $E_\gamma \leq 2000$ keV, ± 0.5 keV for $2500 \leq E_\gamma \leq 5400$ keV, $\pm$ 2 keV for $E_\gamma \geq 6000$ keV.

[b] Legendre coefficients of the shifted component of the γ-ray line.

4507.3-keV level. The angular distribution of the 4507.3 → 3832.2-keV line is typical of a pure dipole transition. This level decays primarily to the 3832.2-keV 2^+ state, although a 21% branch to the ground state is observed. The present experiment provides a particularly high quality data set for that pure $E3$ decay direct to the ground state. The angular distribution of that line enables definite confirmation of a unique 3^- assignment for this level.

There has been some confusion over the lifetime of the 4507.3-keV level because of the existence of the close 4503.6/4507.3-keV doublet. A Doppler shift attenuation factor of $(F\tau) = 0.018 \pm 0.005$ was obtained from our $E_n = 6.2$ MeV data, which is at the limit of our ability to observe shifts and determine lifetimes. This value is also corrupted by feeding effects. Limits of $2 < \tau < 20$ ps can be set, in agreement with the value [17] of Benczer-Koller of $8.8^{+5.5}_{-2.8}$ ps. More precise results are available from more recent lifetime measurements [24], which yield $\tau = 13 \pm 2.2$ ps.

The latter lifetime, together with our branching ratio, enables us to obtain the reduced $E3$ transition strength for this level. The $E3$ strength found from this lifetime is 4.9 ± 1 W.u. This is the first clear and unambiguous determination of that strength from γ-ray decay information. There is an older result from fast electron scattering [25], $B(E3) = 7 \pm 1$ W.u. Coupling strengths for this excitation have also been determined in proton and neutron scattering experiments [6, 20, 26]. These coupling strengths and conclusions drawn from them are in a later section of this paper, dealing with hadron dependence of collective excitations. A result of these experimental comparisons is that the electromagnetic coupling strength is consistently determined either by γ-ray decay measurements of branching ratios and lifetime, or by electron scattering.

4612.3-keV level. This state was observed to decay only to the 2^+ first excited level; it is not clearly observed in alpha inelastic scattering experiments, suggesting that its collectivity is weak or nonexistent. Tape *et al.* [23] assigned $J^\pi = 3^+$ to the level. Based on the angular distribution, our results support the $J = 3$ assignment.

The 4612.3-keV level has a previously measured lifetime of 1.8 ± 0.6 ps. The present experiment yields an attenuation factor of $F(\tau) = 0.059 \pm 0.010$, and a lifetime of 5.3 ± 0.7 ps. This measurement should well represent the lifetime of the level, since there is little feeding to it. The lifetime yields a very small $M1$ transition probability.

5146.2-keV level. This state is observed to decay only into the 4503.6-keV 4^+ level. The decay was studied in coincidence with exit channel protons by Tape *et al.* [23],

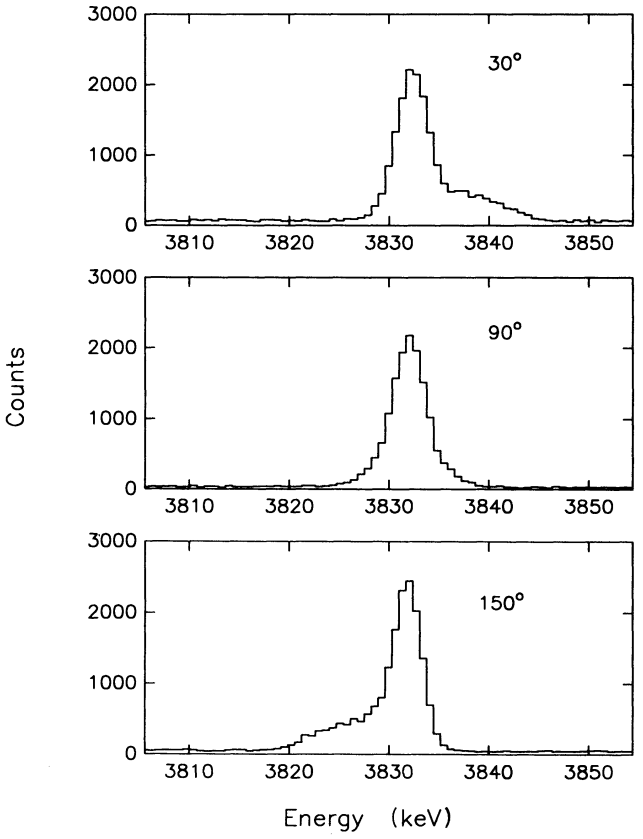

FIG. 4. Line shape for the 3832.2-keV to ground-state γ-ray transition at $E_n = 6.2$ MeV. The large unshifted component is generated from γ-ray feeding to the 3832.2-keV level. This line was analyzed as two separate peaks in order to extract lifetime and INS cross sections.

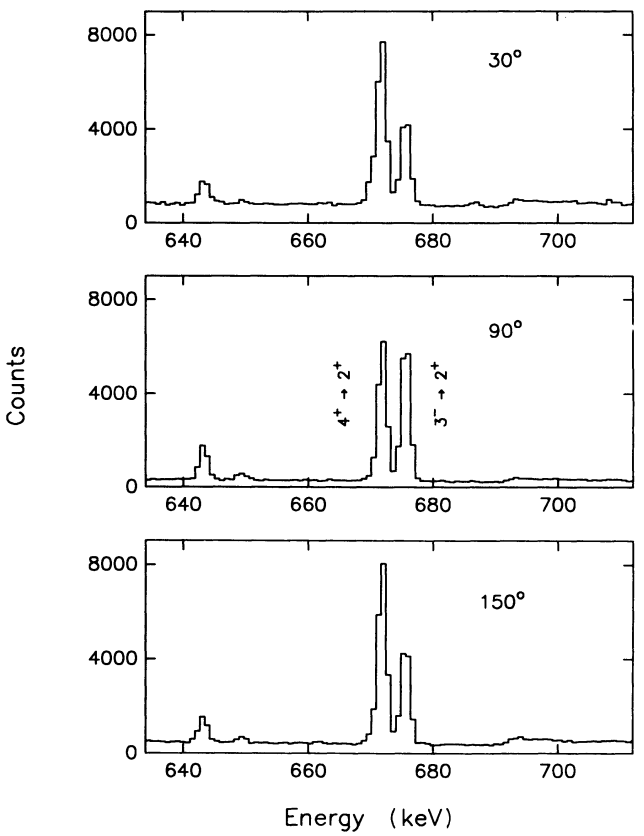

FIG. 5. Transitions from members of the 4.5-MeV doublet to the first excited state appear as adjacent lines in the γ-ray spectrum.

who also concluded that the transition proceeds through the 4503.6-keV level. Previous (p,p') and (e,e') studies suggest $J = 4$ or 5. The state is not clearly observed in alpha inelastic scattering experiments. The 5146.2-keV level was found to be strongly excited in the $E_p = 65$ MeV (p,p') work of Fujita *et al.* [26]. Electron scattering [27] favors a spin and parity assignment of 5^+. The present data indicate the spin should be $J = 3$ or 5. The electron scattering study would have difficulty distinguishing spins of 4 or 5, but clearly discriminates against an assignment of $J = 3$. Combination of experiments requires a spin of 5^+. The mixing ratios established from both the

TABLE V. Levels and cross sections from $E_n = 8.0$ MeV data.

E_x[a] (keV)	J^π	E_γ (keV)	E_f (keV)	Production cross section[b] (mb)	INS cross section (mb)	
3832.2	2+	3832.2	g.s.	706.0(10.9)	111.0(13.1)	[101 ± 9][c]
4283.7	0+	451.6	3832.2	13.6(0.6)	13.6(0.6)	
4503.6	4+	671.4	3832.2	168.4(3.8)	62.2(4.8)	
4507.3	3-	4507.3	g.s.	40.7(3.2)	125(17)	
		675.1	3832.2	162.5(2.7)		
4612.3	3(+)	780.1	3832.2	105.7(1.7)	75.2(3.1)	
5146.2	5+	642.7	4503.6	44.4(1.0)	33.4(1.7)	
5260.9	4(-)	753.8	4507.3	38.0(1.3)	30.5(3.6)	
		648.4	4612.3	6.4(0.4)		
5312.3	2+	5312.2	g.s.	7.3[d](0.6)	57.3(2.4)	
		1480.2	3832.2	47.3(0.8)		
		803.9	4507.3	2.7(0.4)		
5370.0	3-	1537.8	3832.2	37.4(1.5)	56.(2.5)	
		866.9	4503.6	10.7(0.8)		
		862.7	4507.3	11.1(1.1)		
		757.5	4612.3	11.0(1.0)		
5729.6	5-	468.7	5260.9	13.9(0.7)	17.8(2.1)	
		1226	4503.6	8.8(1.9)		
6105.3	(4-)	2273.1	3832.2	2.6(0.3)	21.6(1.0)	
		1597.8	4507.3	19.0(0.9)		
6336.4	2+	6336.4	g.s.	17.1(1.1)	17.1(1.1)	
6345(1)	4+	1841.2	4503.6	24.2(0.9)	33.2(2.4)	
		1733.5	4612.3	4.9(1.1)		
		1199.3	5146.2	4.1(1.9)		
6649(1)	4+	2145.1	4503.6	10.2(1.4)	22.3(1.6)	
		2036.8	4612.3	5.2(0.3)		
		1504.0	5146.2	6.9(0.6)		
6686(1)	2-	2073.9	4612.3	3.0 (1.0)	14.7(1.3)	
		1315.8	5370.0	11.7(0.8)		
6791(2)	(2+)	6791	g.s.	10.8(0.7)	10.8(0.7)	
6807.1	(2+)	2974.8	3832.2	6.6(2.1)	15.8(2.3)	
		2301.9	4503.6	9.2(1.0)		
6830(1)	(3)	2998.7	3832.2	7.3(0.8)	6.6(0.8)	
6896(1)	(2,5)	2389.0	4507.3	8.9(0.9)	12(1.1)	
		1525.7	5370.0	3.1(0.7)		
7008(1)	3-	3175.5	3832.2	27.2(2.2)	33.3(2.3)	
7032	(3,5)	2524.9	4503.6	6.1(0.6)		
7298(1)	(2+)	7298	g.s.	2.1(0.4)	12.2(0.8)	
		3483.9	3832.2	10.1(0.7)		
7370(2)		7370	g.s.	10.7(0.2)	10.7(0.2)	
7440(2)	(2+)	7440	g.s.	2.4(0.5)	2.4(0.5)	
7498(1)	(3)	1767.8	5729.6	4.9(0.6)	4.9(0.6)	
7569(2)		3736.6	3832.2	6.2(3.8)	6.2(3.8)	
				Total INS =	1660.4 ± 14.4 mb	

[a]Uncertainties in level energies are typically $\approx \pm$ 0.5 keV except where noted.

[b]Tabulated uncertainties reflect statistical only. An additional uncertainty of $\sim$ 8% is determined principally by uncertainties in the ^{12}C cross sections used for calibration.

[c]Value determined from the Doppler-shifted component of the 3832-keV line.

[d]Cross section of this γ-ray corrected for the contribution from the second escape peak of the 6336-keV γ-ray line. See text.

6.2 and 8.0 MeV angular distributions are in excellent agreement; the decay can only be a pure $M1$ transition.

5260.9-keV level. The 5260.9-keV level is observed to decay to the 4507.3-keV 3^- and 4612.3-keV 3^+ levels. The ^{48}K β-decay experiments have suggested 4^- for this level based on logft values. The level is not observed in (α,α') experiments [21]. Analysis of the 65 MeV (p,p') data [26] did not give a good quality fit for $J = 4$. They propose a 5^+ assignment. However, our angular distribution for the 5260.9 → 4612.3-keV level completely rules out that assignment, which would call for an $E2$ decay. The angular distributions show pure dipole transitions to both the 3^+ and 3^- levels. Fits to the angular distributions of both gamma decay modes in the present data indicate $J^\pi = 4^-$ as the only possibility when these data and the β-decay results are combined.

5312.3-keV level. The ENDSF database accepts states at 5304 ± 6 and 5322 ± 10 keV, but only one state is seen in the present work. The level at 5312.3 keV decays to the 0^+ ground state, 2^+ first excited state, and the 4507.3-keV 3^- state. This level was not clearly observed in the $E_p = 65$ MeV (p,p') data nor was it observed in the (α,α') measurements. These facts are consistent with it being a level with very little collective strength. The χ^2 fits to the 1480.2-keV transition allow spin assignments from 2 to 4, but the observation of the transition to the ground state requires $J = 2^+$. Using these two transitions the energy of the level can be fixed at 5312.3 keV. This is the first observation of the 5312.3 → ground-state transition.

The lifetime of the 5312.3-keV state is measured with the transition to the first excited state. There is no feeding to this level from any states $E_x < 8$ MeV; therefore the lifetime measurement is free of ambiguities. The average attenuation factor of $F(\tau) = 0.53 \pm 0.03$ corresponds to a lifetime of 335^{+40}_{-20} fs.

The 5312.3-keV peak in the detector spectrum measured at 8.0 MeV neutron energy contains a contribution from the second escape peak of the 6336.4-keV transition. The production cross section for this gamma ray in Table V was corrected using the branching ratios determined from the 6.2-MeV data.

5370.0-keV level. This state is strongly excited in (p,p') and (α,α') experiments, suggesting substantial collectivity. Our data confirm [20] the previous 3^- spin assignment. The level is observed to decay to the 3832.2-keV 2^+, 4503.6-keV 4^+, 4507.3-keV 3^-, and 4612.3-keV 3^+ states. The $E1$ transitions dominate the decay of this 3^- level.

The transition at 757.5 keV was difficult to place. It could have been either the 5260.9 → 4503.6-keV or the 5370.0 → 4612.3-keV transition. The question was resolved by determining the excitation threshold of that line. The ^{48}Ca$(n,n'\gamma)$ excitation function was measured at 90° from $E_n = 5.35$ to 6.20 MeV in nine steps. The excitation function for the 757.50-keV line was then compared to those for 5260.9 → 4507.3 and the 5370.0 → 4503.6-keV lines. From the shape of the excitation functions near threshold [28], we conclude that the 757.5-keV transition must originate from the level at 5370.0 keV.

6105.3-keV level. The 6105.3-keV level decays to the 3832.2-keV 2^+ and 4507.3-keV 3^- levels. The combination of (α,α') and (e,e') [27] data indicate negative parity and spin 4. This assignment leads to a surprisingly strong $M2$ transition from this level to the 2^+ level—such multipolarity transitions are seldom observed. The present data are insensitive to the spin of this level; thus we cannot confirm the spin assignment.

6336.4-keV level. A transition of 6336.4 keV is evidence for a new level at this energy. The large Doppler shift observed $[F(\tau) = 0.54]$ corresponds to a lifetime of 276 ± 40 fs. From the measured lifetime alone, the spin may be restricted to $J^\pi = 1^\pm$, or 2^+ using the recommended upper limits [29] for reduced transition probabilities in the mass $A = 45$–90 region. The positive a_2 coefficient of the Legendre polynomial expansion of the angular distribution requires a spin of 2^+.

***6345-keV level.* This level has been assigned $J^\pi = 4^+$ from (p,p'), (α,α'), and (e,e') reactions. The angular distributions of the deexcitation γ rays are not sufficiently precise to indicate a spin. An 1841.2-keV transition is observed to the 4503.6/4507.3 keV doublet. Based on the level energy obtained using the transitions to the 4612.3- and 5146.2-keV states, the 1841.2-keV transition proceeds into the 4503.6-keV, 4^+ level.**

6649-keV level. All previous experiments have indicated a 4^+ spin assignment for this level. The decays to the 4503.6-keV 4^+ and 4612.3-keV 3^+ levels have negative a_2 Legendre coefficients. This means that the angular distributions are those of either dipole or mixed dipole/quadrupole transitions. The angular distribution of the 1504.0-keV γ ray to the 5146.2-keV state suggests a spin assignment of 4 or 6, but a spin of 6 is impossible, since this would imply a positive a_2 coefficient for the decay into the 4^+ level. It is also highly unlikely that a spin-6 state would decay into a 3^+ level. We confirm the previous spin-4 assignment. The ^{48}K β-decay experiment [22] has indicated a 1278-keV decay into the state at 5370.0 keV; however, this transition is not observed in the present experiment.

6791-keV level. A level at 6794 ± 7 keV is described as clearly observed in (p,p') [26] experiments, excited with a momentum transfer of $L = 2$. Wise *et al.* [27] observe a state at 6796 ± 7 keV, but are not able to provide a firm spin assignment, proposing 1^- or 2^+. In the present experiment, the angular distribution of the deexcitation γ ray to the ground state has an $a_2 < 0$, and this is compatible only with $J^\pi = 1^-$. This short lived state has a lifetime $\tau < 10$ fs; its Doppler shift is maximal.

6807-keV level. A transition of 2974.8 keV appears in the spectra above a bombarding energy of $E_n \sim 6.8$ MeV. From energy differences between known levels, the only possible originating levels would be at 7469, 7498, or 7569 keV. Judging from the excitation function, it is unlikely that this line belongs to any of these three levels—its energy threshold is much too low. A new level is thus indicated at an excitation energy of 6807 keV. Fortunately, this placement accounts for the presence of another new line observed here.

A transition of 2301.9 keV appears in the excitation function above $E_n \sim 6.8$ MeV. Candidates for the source of this line are transitions between the levels 6791 →

4612.3 keV and 6896 → 4503.6 keV. However, in neither case does the energy difference between levels agree with the observed transition energy of 2301.9 keV. The energy difference and threshold are consistent with a cascade from the newly placed 6807-keV level to the 4503.6-keV level.

Transitions are observed from this new level to the first excited state and the 4503.6/4507.3-keV doublet as discussed above. Angular distributions are not sufficiently sensitive to indicate a spin for this level. The presence of the levels at 6791 and 6807 keV may resolve the disagreement between (p,p') and our results mentioned in the discussion for the 6791-keV level. The (p,p') angular distribution may actually be to this new level, which would then indicate 2^+ as the appropriate assignment.

6830-keV level. The angular distribution of the decay into the first excited state suggests $J = 3$. This is supported by the (p,p') work of Fujita *et al.* [26], who see an $L = 3$ excitation at this energy.

6896-keV level. The combination of previous experiments has suggested a doublet at this energy. The β-decay experiments indicate a 2^- level at $E_x = 6895$ keV. Electron scattering data indicate a 5^+ level at $E_x = 6893$ keV. The 65-MeV (p,p') data are consistent with a mixture of 2^- and 5^+. In the present experiment two transitions (2338 and 1525 keV) are observed from the 6896-keV level to 3^- states, and the angular distributions of both γ rays are consistent with transitions of $L = 1$ multipolarity, even though the uncertainty is rather large for the a_2 coefficient of the 1525-keV transition. This would indicate a spin assignment between 2 and 4, which would eliminate the 5^+ possibility. Two additional transitions to the 4612.3 and 3832.2-keV states seen in β decay are too weak to be observed in this work. There is no evidence for a doublet in the present $(n,n'\gamma)$ data.

7029-keV level. Deexcitations to the 4503.6-keV 4^+ and 5260.9-keV 4^- states have been observed in $(p,p'\gamma)$ experiments. The angular distribution of the 2524.9-keV line has a large negative a_2 coefficient, which permits spin assignments of $J = 5$ or 3 (with large $L = 2/L = 1$ mixing ratios). The 1769-keV transition to the 5260.9-keV state is not observed in the present experiment, at a sensitivity of $\sigma \sim 3$ mb. The 7029-keV state was not clearly observed in (p,p') scattering [26].

7298-keV level. The level has been assigned 3^- from (p,p') experiments, although electron scattering has suggested (1^-). We observe a strong ground-state decay as well as a branch to the first excited state. The strong positive a_2 Legendre coefficient of the ground-state decay indicates spins of 2^+ or 3^-. The large uncertainty of the a_2 coefficient results from the seriously diminished detector efficiency at that elevated γ-ray energy, together with the small sample. This prevents us from clearly discriminating between these two possible assignments using only anisotropies. The measured lifetime of $\tau < 10$ fs yields a ground-state transition strength of $B(E2) > 0.064$ W.u. if 2^+ and $B(E3) > 201$ W.u. if 3^-. Based on recommended upper imits for $E3$ decay in the $A = 45$–90 region [29], the spin is restricted to $J = 2^+$.

7440-keV level. The level at 7440 keV was seen to decay to the ground state in this and the $(p,p'\gamma)$ experiments. The level is not observed in higher energy (p,p') and (e,e') experiments. The decay to the ground state has a very large $a_2 = 1.7 \pm 0.7$, which indicates either $J = 2^+$ or 3^-. Based on recommended upper limits for $E3$ transition strengths in the $A = 45$–90 mass range [29], this level must be assigned 2^+.

7498-keV level. This level has only previously been observed in 160 MeV (p,p') data [30], where the analysis has indicated $J = 3$. Decay is observed in the present experiment to the 5730-keV 5^- state via a γ ray with very large a_2 and a_4 coefficients in its angular distribution, which calls for a spin $J \geq 3$.

7569-keV level. A level at 7569 ± 10 keV has been suggested from $(p,p'\gamma)$ experiments. In the present experiment only γ decay to the 3832.2-keV first excited state is observed. Thus its spin $J \leq 4$.

IV. STRUCTURE INTERPRETATIONS

A. Collective excitations from neutron and γ-ray detection

Differential (n,n') cross sections were measured previously [6, 7] at $E_n = 8.0$ MeV to the 3832.2-keV 2^+ first excited state, the 4283.7-keV 0^+ state, and the cluster of states at 4503.6/4507.3/4612.3 keV. Only the present γ-ray detection experiments, which yield angle-integrated neutron scattering cross sections, have been able to resolve the cluster of three levels at $E_x \approx 4.5$ MeV, which includes the collective 3^-_1 level. The present experiment, with its 2-keV energy resolution, provides separate cross sections for each member of the triplet, confirming the measured cross sections and analyses of them made in the earlier study [6]. The separation enabled us to affirm that the sum of the two neutron-induced $E3$ amplitudes to the two 3^- levels of ^{48}Ca is within 25% of that of the single 3^- level in ^{40}Ca.

One of the key points of the earlier neutron scattering study [6] was the splitting of the octupole strength between the two 3^- levels at 4507.3- and 5370.0-keV excitation energies. This splitting had not been noted prior to our two neutron scattering studies. Another of the goals of the present study was testing neutron and proton scattering strengths versus electromagnetic $E2$ and $E3$ strengths for several levels through examination of reduced transition rates and elastic and inelastic scattering intensities. One might note that an electron scattering experiment [27] shows the ratio of $E3$ excitation strengths to the second 3^- level to that of the first 3^- level to be about 0.16, whereas in the neutron scattering experiment [6] the same ratio was found to be 0.67.

Lifetime measurements for levels of ^{48}Ca reflect electromagnetic strengths; these are presented in Table VI for many levels. Lifetimes not available from the present experiment are supplemented from the literature. Because our $E2/M1$ mixing ratios are generally consistent with zero, the reduced electromagnetic transition strengths are calculated assuming pure multipolarities.

TABLE VI. Lifetimes and transition strengths in ^{48}Ca.

E_x (keV)	Assumed J^π	F^a	τ^a (ps)	E_γ (keV)	J_f	σL	$\|M\|^2$ (W.u.)^b
3832.2	2+	0.84(3)	$0.060^{-0.012}_{+0.011}$	3832	0+	$E2$	$1.6^{+0.4}_{-0.3}$
4283.7	0+		332 ±16^c	452	2+	$E2$	9.8 ±0.5
4503.6	4+		1960 ±25^c	671	2+	$E2$	0.31±0.4
4507.3	3-	0.018(5)	13 ±2^c	675	2+	$E1$	$1.4^{+0.3}_{-0.2}$ E-4
				4507.3	0+	$E3$	$6.5^{+1.1}_{-0.9}$
4612.3	3+	0.054(10)	$5.3^{-0.6}_{+1.3}$	780	2+	M 1	$0.013^{+0.002}_{-0.002}$
5146.2	5+		< 700^c	643	4+	$M1$	> 1.7 E-4
5260.9	4+	0.042(7)	$7.3^{-1.1}_{+2.0}$	754	3-	$M1$	$8.7^{+1.6}_{-2.0}$ E-3
				648	3+	$E1$	$5.2^{+0.9}_{-1.1}$ E1-5
5312.3	2+	0.53(3)	$0.335^{-0.019}_{+0.040}$	5312	0+	$E2$	$7.2^{+0.4}_{-0.8}$ E-3
				1480	2+	$M1$	$1.6^{+0.7}_{-0.9}$ E-2
						$E2$	$1.8^{-1.6}_{+38.}$ E-4
						($\tan^{-1}\delta$=0.6±0.4)	
				803	3-	$E1$	$2.1^{+0.1}_{-0.2}$ E-4
5370.0	3-	0.11(1)	$2.6^{-0.2}_{+0.2}$	1537	2+	$E1$	$4.1^{+0.3}_{-0.3}$ E-5
				867	4+	$E1$	$7.4^{+0.6}_{-0.5}$ E-5
				863	3-	$M1$	$2.9^{+0.2}_{-0.2}$ E-3
				753	3+	$E1$	$1.0^{+0.1}_{-0.1}$ E-4
5729.6	5-	0.19(6)	$1.3^{-0.3}_{+0.7}$	469	4-	$M1$	$0.15^{+0.04}_{-0.05}$
				1226	4+	$E1$	$1.2^{+0.4}_{-0.5}$ E-4
6105.3	4-	0.73(6)	$0.200^{-0.040}_{+0.025}$	1598	3-	$M1$	$3.4^{+0.9}_{-0.4}$ E-2
				2273	2+	$M2$	$3.0^{+0.3}_{-0.6}$ E-2
6336.4	2+	0.54(4)	$0.276^{-0.041}_{+0.041}$	6336	0+	$E2$	$2.8^{+0.5}_{-0.4}$ E-2
6345	4+	0.66 (3)	$0.260^{-0.018}_{+0.050}$	1841	4+	$M1$	$1.4^{+0.1}_{-0.2}$ E-2
				1733	3+	$M1$	$3.5^{+0.3}_{-0.5}$ E-3
				1199	5-	$E1$	$2.0^{+0.2}_{-0.3}$ E-4
6649	4+	0.75(7)	$0.164^{-0.040}_{+0.060}$	2145	4+	$M1$	$9.0^{+2.9}_{-2.4}$ E-2
				2036	3(+)	$M1$	$5.3^{+1.7}_{-1.4}$ E-3
				1504	5-	$E1$	$4.1^{-1.3}_{+1.1}$ E-4
6686	2-	0.85(11)	$0.100^{-0.075}_{+0.080}$	2073	3(+)	$E1$	$1.7^{-5.0}_{+0.7}$ E-4
				1315	3-	$M1$	$0.11^{-0.32}_{+0.05}$
6791	2+	1.05(3)	< 0.010	6791	0+	$E2$	> 0.53
6807	?	0.74(11)	$0.120^{-0.055}_{+0.063}$	2975	2+		
6896	2+^{d}	0.86(15)	$0.080^{-\inf}_{+0.120}$	2388	3-	$E1$	$5.0^{+\inf}_{-3.0}$ E-4
				1525	3-	$E1$	$6.9^{+\inf}_{-4.2}$ E-4

TABLE VI. (*Continued*).

E_x (keV)	Assumed J^π	F[a]	τ[a] (ps)	E_γ (keV)	J_f	σL	$\|M\|^2$ (W.u.)[b]
7008	3-	0.84(4)	$0.100^{-0.020}_{+0.025}$	3175	2+	$E1$	$2.3^{+0.6}_{-0.5}$ E-4
7298	2+	1.02(3)	< 0.010	7298	0+	$E2$	> 0.064
				3484	2+	$M1$	> 1.5 E-3
7440	2+	0.59(1)	$0.256^{-0.010}_{+0.010}$	7440	0+	$E2$	$1.34^{+0.05}_{-0.05}$ E-2

[a] F values given are from the present experiment. Lifetimes are those determined from the present experiment's $F(t)$, except where noted.

[b] Reduced transition strengths are expressed in Weisskopf units, or single-particle speeds. Except where noted, values are calculated assuming a pure transition (δ=0).

[c] Lifetimes taken from ENDSF.

[d] Assumed $J = 2^+$, since decays occur into two 3^- states.

B. Neutron scattering cross section comparisons

Comparisons of the measured (n, n') and the present inferred neutron inelastic scattering cross sections for many levels is presented in Table VII. The agreement is remarkably good. The excellent normalization accuracy of the neutron detection experiment [6, 7] led to much smaller uncertainties, as is evident in Table VII. However, only statistical uncertainties and cascade feeding corrections affect the ratios of cross sections within the three level cluster near 4.5 MeV, for instance, in the present γ-ray detection experiment. As is evident in Table V, those uncertainties are quite modest. Thus we use the γ-ray cross sections to separate levels in unresolved groups, but rely on the neutron detection measurements for absolute normalization. This yields the best cross-section accuracy, which is important for the discussions to follow.

A second goal for the present experiment is to compare the experimental INS cross sections to those generated by a coupled-channels potential analysis [6, 7] of neutron scattering cross sections from ^{48}Ca. The work by Hicks *et al.* sought to study the role of collective excitations in ^{48}Ca by using a dispersive coupled-channels optical model analysis of neutron scattering for neutron energies from a few keV to 20 MeV. Such analysis requires knowledge of neutron scattering cross sections to those states expected to have collective strengths, i.e., the 3832.2-keV 2^+ and two 3^- levels, as well as states only excited through the compound system mechanism [31]. These latter cross sections and mechanisms are important for noncollective levels, in order that the compound system and direct coupling mechanisms can be accurately separated for the collective levels, where both mechanisms are important.

Comparisons of measured cross section with coupled-

TABLE VII. Cross-section comparisons at E_n = 8.0 MeV.

	ECIS79 Cross sections		Experimental cross sections	
Level	Total INS (mb)	Compound (mb)	$(n, n'\gamma)$ (mb)	(n, n') (mb)
0		67		
3832.2	105	72	101.(9)	101.(2)
4283.7	17	17	13.6(1)	11.7(2)
4503.6	59	59	62.2[a](5)	
4507.3	96	58	125[a](17)	248.(4)
4612.3	68	68	75.2[a](3)	
5147	43	43	33.4(2)	
5260.9	57	57	30.5(4)	
5312.3	60	60	57.3(2)	
5370	71	52	56(6)	
5460	15	15		
5730	45	34	17.8(6)	

[a] The sum of these values corresponds to the 248 mb measured in the neutron detection experiment of Ref. [6].

channels calculations of them [7] are also given in Table VII. The compound system or statistical-model cross sections were calculated with the computer code OPSTAT [32], which included Tepel-Hoffman-Weidenmuller width fluctuation and channel-correlation corrections [31]. All levels up to an excitation energy of 8-MeV, the maximum incident energy, were included to be certain of a proper statistical distribution of flux for states up to 8 MeV excitation. The potential parameters of Hicks *et al.* were then used as input to the coupled channels code ECIS79 [33] to predict the contribution from direct excitation. Vibrational phonon coupling strengths β_l in Hick's analysis [7] were $\beta_{2_1} = 0.08 \pm 0.01$, $\beta_{3_1} = 0.15 \pm 0.01$, and $\beta_{3_2} = 0.10 \pm 0.02$.

The large amount of γ-ray feeding to the 4507.3-keV state does create a particularly large uncertainty for our inferred cross section to that level. This uncertainty does not weaken the strength of the comparisons between the two experiments, however, because the inelastic scattering cross section to the whole three-level cluster is well determined in the neutron detection experiment [6], and the separate cross sections to the 4^+ and 3^+ members of the triplet are well measured. Thus the cross section to the 3_1^- level is well fixed. The 2^+ and 3^- levels at 3832.2 and 4507.3 keV have quite substantial collective components in their measured cross sections. No collective coupling strength is required for the 4503.6-keV 4^+ level, as had also been projected in an earlier (^{3}He,^{3}He$'$) experiment [34].

The agreement between the two neutron scattering experiments and the combined cross-sections model is not as good for the 5370.0-keV second 3^- and 5729.6-keV 5^- levels; there is some unavoidable uncertainty in the compound system cross sections as one goes to levels of higher excitation energy within the framework of the combined, two reaction mechanism model. Fortunately the fixing of the octupole strength for the second 3^- level, β_{3_2}, did not depend upon this complex model-measurement cross-section comparison. That coupling strength had to be precisely fixed in order to represent the virtual coupling required fitting low-energy resonance structure in neutron scattering [6]. The 5729.6-keV 5^- state shows little or no direct coupling contribution at this incident energy; it does not figure in further analyses.

C. Proton vs neutron particle-hole structures for collective levels

The probe dependence of excitation of both the 2_1^+ and the two 3^- levels allows us to project the relative strengths of neutron particle-hole (ph) and proton p-h amplitudes. Often these probe-dependent excitation amplitudes are characterized in terms of the β values which are used in strong coupling models of their excitations. We have chosen to express all strengths in these terms, converting lifetimes and reduced electromagnetic strengths to these parameters. Scattering amplitudes are proportional to the product βR, and reduced electromagnetic strengths from lifetimes are proportional to βR^L, where L is the transition multipolarity. Thus a choice of R, the interaction radius, must be made. For these comparisons, we have chosen $R = rA^{1/3}$, with $r = 1.24$ fm, consistent with the value used in the earlier neutron scattering study [6] at 8 MeV, and A is the atomic mass.

The interpretive procedure we use depends upon, and only upon, ratios of excitation amplitudes for different probes, or upon the reduced matrix element ratios. Such matrix element ratios are just the square root of reduced transition probabilities; when both excitation strengths we wish to compare are quoted in W.u., no β values need be inferred; we can compare the matrix elements directly.

The comparison we make of excitation strengths with different probes is based on a formulation derived from the study of core polarization effects and differences in deformation parameters, β. The formulation was developed by Brown, Madsen, and collaborators [35, 36]. A similar study in the same spirit using different notation was made by Alons *et al.* [37], and our notation is similar to that of the last cited reference. The matrix element for proton scattering to a collective excitation is given by

$$M_{pp'} = (\chi_{pp} M_p + \chi_{pn} M_n)/(\chi_{pp} Z + \chi_{pn} N)$$

with a similar equation for the neutron scattering amplitude, $M_{nn'}$, including appropriate changes of subscripts. The parameters χ_{pp} and χ_{pn} are weight factors for the strengths of the effective proton-proton and proton-neutron interactions, respectively. The M_p and M_n are target-proton and -neutron excitation amplitudes, respectively. Thus the electromagnetic excitation amplitude is just $M_{\rm em} = M_p$, since only target protons are excited directly. It is well known that $\chi_{pn} = \chi_{np} \approx (2.5 - 3)\chi_{pp}$, and that $\chi_{pp} = \chi_{nn}$. Bernstein, Brown, and Madsen [36] advance persuasive arguments that in our projectile energy regimes, $\chi_{np} \approx 3\chi_{pp}$. This same strength ratio is found by Alons *et al.* using slightly different arguments [37]. We have used this ratio throughout our analyses, but fortunately our results are not sensitive to the precise value used. The scattering matrix elements are normalized not only for the different nucleon-nucleon effective interaction strengths, but also to the numbers of protons Z and neutrons N.

This normalization means that for a deformed rotor M_n/M_p would be just N/Z, and $M_{nn'} = M_{pp'} = M_{\rm em}$, or, equivalently, all three beta values, $\beta_{nn'}$, $\beta_{pp'}$, and $\beta_{\rm em}$, would be equal, as indeed has been found for deformed nuclei [38].

The present comparisons only involve ratios of beta values or scattering amplitudes; we can write, for the ratio

$$\frac{\beta_{pp'}}{\beta_{nn'}} = \left(\frac{1 + \chi M_R}{1 + \chi(N/Z)}\right)\left(\frac{\chi + (N/Z)}{\chi + M_R}\right),$$

where M_R is the target-nucleon excitation-amplitude ratio M_n/M_p and χ is the ratio χ_{np}/χ_{pp}. For α-particle scattering all χ values are 1; we can then write

$$\frac{\beta_{\alpha\alpha'}}{\beta_{\rm em}} = \frac{(M_p + M_n)/(Z + N)}{M_p/Z} = \frac{1 + M_R}{1 + (N/Z)}$$

for the ratio of α-particle scattering to electromagnetic amplitudes.

The first test of these ratios, and the inferred struc-

tures of collective levels, is for the first excited 2^+ level at 3832.2 keV. The proton scattering amplitude is obtained as an average of two rather consistent values, the older one [20] of Gruhn *et al.* at 12-MeV incident, and the recent one [26] of Fujita *et al.* at 65 MeV. Together with the neutron amplitude [6] we find $\beta_{pp'}/\beta_{nn'} = 0.14/0.09 = 1.55$. This leads to the rather startlingly large ratio $M_R = 3.8$. Such a large result for this level had been found much earlier [36], without either the 65-MeV proton scattering results of Fujita *et al.* or the neutron scattering results [6] having been available at that time. Thus this work nicely confirms the anomalously large ratio.

This large M_R ratio can be tested by examining the ratio of α scattering to electromagnetic excitation. The presently determined 2^+ lifetime of Sec. III agrees with that earlier determined [24]; this gives a reduced $E2$ strength of 1.7 W.u. The early α scattering results provide the much larger value of 4.9 W.u. [21]. Thus an experimental ratio of $\beta_{\alpha\alpha'}/\beta_{\rm em} = \sqrt{4.9/1.7} = 1.7$ is found. Alternatively, based on the ratio M_R of 3.8 above, we would expect this latter ratio to be 2.0, which is quite good agreement. All of the experimental information is consistent, and suggests neutron p-h amplitudes are quite dominant for this first 2^+ level.

This ratio had been cited [36] as the singularly largest one reported for any nucleus. The value of 2.7 times N/Z means that more than 70% of the wave-function amplitude corresponds to neutron p-h amplitudes, and less than 30% to proton excitations. As noted earlier [4, 36], such strong neutron excitations could correspond to the fact that even parity states can be constructed easily by neutron excitations from the filled $f_{7/2}$ shell into the f-p shell, whereas proton excitations must cross the entire $f_{7/2}$ and f-p shells to reach the $g_{9/2}$ orbit.

The excitation strengths for the 3_1^- level present a rather different picture. The $E3$ strength of 4.9 W.u. from the lifetime of the 4507.3-keV level leads to a $\beta_3 = 0.16 \pm 0.015$. The electron scattering result [25] for collective strength leads to a $\beta_3 = 0.19 \pm 0.02$. Accuracy and directness of interpretation favors the lifetime result; we take the value $\beta_3 = 0.17$ as most representative of the electromagnetic excitation value. The neutron scattering study provided the value $\beta_3 = 0.15 \pm 0.01$. Finally several proton scattering experiments produce values of β_3 ranging from 0.15 to 0.17, tending to be slightly larger than the neutron scattering result. Thus there is a suggestion that the neutron scattering amplitude is about 7% weaker than the electromagnetic or proton scattering amplitude. Alternatively, within errors, one could not rule out the suggestion that all particles see about the same strength. The finding that all probes see about the same strength leads directly to the conclusion that $M_n/M_p \approx 1.4$, or the ratio of N/Z, and thus that the p-h amplitudes per proton and per neutron are roughly of the same strength for this 3_1^- level.

The most recent measurements of transition rates are for the lifetime of the 3_1^- level and the neutron scattering amplitude. These results suggest that the ratio $M_{\rm em}/M_{n,n'} \approx 0.17/0.15$. This leads to $M_n/M_p \approx 0.5 - 0.6$. Thus, as Jaffrin and Ripka (JR) had found in their model calculations [4], proton p-h amplitudes would dominate the 3_1^- excitation, but not dramatically; the present comparisons suggest that neutron p-h amplitudes are about half to two-thirds as strong as proton, rather than being one-fourth as strong [4], as found in the JR calculations.

The splitting of octupole collective strengths in ^{48}Ca has been studied only in electron and neutron scattering, with strength information also implied by γ-ray decay strengths. A large electromagnetic $E3$ strength in the 5370.0-keV 3_2^- level would depend specifically on large proton p-h components in the state—were that so, one might expect to see a direct decay to the ground state. The measured lifetime can be used to set an upper limit on the branching ratio for this $E3$ transition as follows: the fastest $E3$ transitions in the $A = 45$–90 mass region [29] have $B(E3) \sim 25$ W.u. Requiring the calculated $B(E3)$ for the 5370.0-keV to ground-state transition to be less than this value sets the ground state branch to less than 65%—an amount which should be easily observable. This decay branch is not observed in the present experiment at a level of $\sim 3\%$, which suggests a reduced $E3$ strength < 1.3 W.u. Actually, the electron scattering strength noted below [27] suggests an $E3$ strength ~ 0.8 W.u., well consistent with our non-observation of direct decay to the ground state.

Electron scattering shows an intensity to the second 3^- level only about 16% that to the 3_1^- level [27]. This

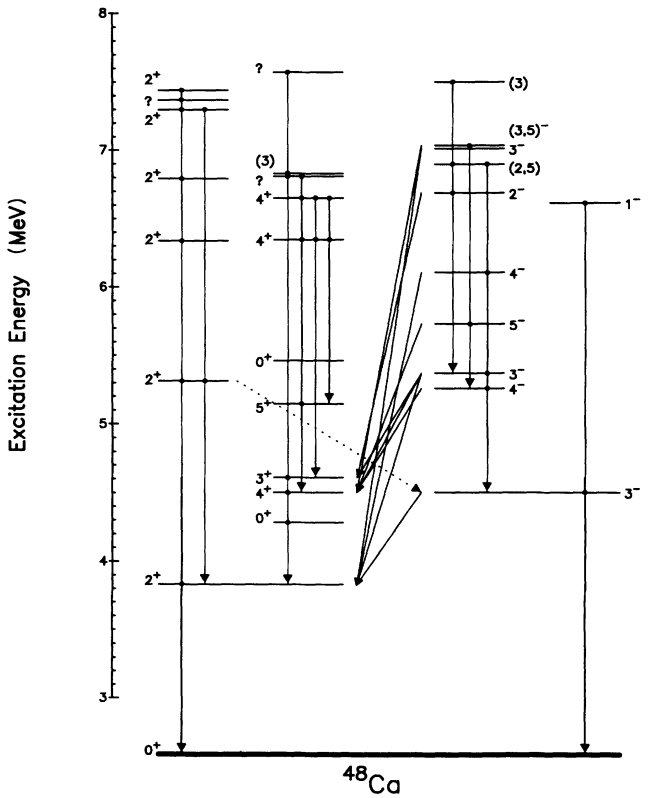

FIG. 6. Gamma-ray decay scheme for ^{48}Ca, illustrating the different decay patterns of even- and odd-parity levels.

yields an amplitude ratio for electron scattering to the two levels of 2.4. In contrast, the neutron scattering experiment found [6] an amplitude ratio of only 1.5. With these very different ratios being determined, we can calculate the ratio of target neutron excitations to proton excitations for this level to be $M_n/M_p \approx 3$. Thus for the 3_2^- level, neutron excitations are dominant, which is why it is weakly excited in electron scattering compared to neutron scattering, and why its collective character has been little marked. This is in contradiction to the findings of the JR calculations, as well.

These fairly striking probe dependencies for collective excitations of ^{48}Ca are in marked contrast to findings in ^{40}Ca, as should be the case. Since ^{40}Ca is a self-conjugate nucleus, its excitations should be probe independent, indicating that all levels have the same proton as neutron p-h excitation amplitudes. This is indeed found for the lowest two 2^+ levels and for the lowest 3^- octupole excitation in ^{40}Ca. Within uncertainties $\beta_{nn'} \approx \beta_{em} \approx \beta_{p,p'}$ for all excitations [39].

The odd-parity proton p-h splitting is about 6 MeV, from the filled *s-d* shell to the $f_{7/2}$ shell. For neutrons in ^{48}Ca the splitting is closer to 8 MeV, since the $f_{5/2}, p_{3/2}$, and $p_{1/2}$ subshells must be skipped to get an odd-parity excitation [4], or one must excite from the $f_{7/2}$ shell to the $g_{9/2}$ shell. Thus it is natural to expect two 3^- levels split apart by about 2 MeV. On these grounds we would expect the lowest 3^- level to be dominated by proton excitations, and the higher energy 3^- excitation would have a much larger neutron component—it would thus be substantially more strongly excited in neutron scattering than in electromagnetic excitation. This is just the case experimentally. The two experimental 3^- levels are separated by only about 0.9 MeV, however, rather than the expected 2 MeV, perhaps indicative of mixing of the proton and neutron excitations, particularly in the 3_1^- level.

The complete gamma-decay scheme of ^{48}Ca is shown in Fig. 6. States are divided into several classifications: positive-parity states that decay directly to ground, negative-parity states that decay directly to ground, and then other positive- and negative-parity states. Several interesting trends may be noted. There are no transitions from positive-parity to negative-parity states. The interpretation may rest on the likelihood that positive-parity states are heavily dominated by neutron p-h excitations, as we have found for the 2_1^+ level. The odd-parity levels are more likely to be mixed proton and neutron p-h configurations. Thus they are as likely to decay to the neutron configurations of the positive-parity levels as to decay internally. The dominantly neutronlike positive-parity levels would connect most rapidly to each other. Jaffrin and Ripka [4] and Gmitrová *et al.* [40] have performed 1p-1h RPA calculations for the negative-parity states in ^{48}Ca. The spectrum of negative-parity levels is reproduced very well. Calculations of positive-parity states have met with little success [4, 41–43].

V. SUMMARY

Inelastic neutron scattering has been used to study the excited states of ^{48}Ca below $E_x = 7.6$ MeV. Evidence was found for three previously unobserved levels. Angular distributions were analyzed to extract definite, unique spin assignments for nine previously unassigned levels. Through γ-ray excitation functions measured at 90° and through γ-ray angular distributions, both production cross sections and γ-ray branching ratios have been determined. Use of an high-purity Ge detector enabled the doublet at $E_x = 4.5$ MeV to be cleanly separated, and definite spin assignments made to both members. Lifetimes and electromagnetic transition rates were determined for 20 levels using the Doppler-shift attenuation method. Angle-integrated neutron scattering cross sections inferred from the data support the collective strengths found for low-lying states in a recent neutron-detection experiment. The comparison of neutron, proton, and α-particle scattering strengths with electromagnetic decay rates has demonstrated that the first excited 2^+ level and second 3^- levels are dominated greatly by target-neutron excitations, while the 3_1^- level probably has modest dominance of proton p-h excitations. These structural differences, if they can be generalized from the few states studied, may explain why odd-parity levels decay to each other and to even-parity levels, while even-parity levels tend to decay only to each other.

ACKNOWLEDGMENTS

The authors would like to thank Dau-Wei Wang, Tamás Belgya, and Bela Fazekas for many helpful discussions on neutron scattering and Doppler shift attenuation analysis. This work was supported by the National Science Foundation under Grants No. PHY-8702369 and PHY-9001465.

[1] E. Kashy, A. Sperduto, H. A. Enge, and W. W. Beuchner, Phys. Rev. **135**, 865 (1964).
[2] W. D. Metz, W. D. Callender, and C. K. Bockelman, Phys. Rev. C **12**, 827 (1975).
[3] K. Lips and M. T. McEllistrem, Phys. Rev. C **1**, 100 (1970); K. Lips, *ibid.* 4, 1482 (1971).
[4] A. Jaffrin and G. Ripka, Nucl. Phys. **A119**, 529 (1968).
[5] J. A. Harvey, C. H. Johnson, R. F. Carlton, and B. Castel, Phys. Rev. C **32**, 1114 (1985); R. F. Carlton, J. A. Harvey, R. L. Macklin, C. H. Johnson, and Boris Castel, Nucl. Phys. **A465**, 274 (1989).
[6] Sally F. Hicks, S. E. Hicks, G. R. Shen, and M. T. McEllistrem, Phys. Rev. C **41**, 2560 (1990).
[7] Sally F. Hicks, Neutron Scattering Studies on the Doubly Magic Calcium Nuclei, ^{40}Ca and ^{48}Ca, in the Low Energy Resonance Region, Ph.D. dissertation, University of Kentucky (1988).
[8] G. W. Phillips and K. W. Marlow, Nucl. Instrum. Methods **137**, 525 (1976).
[9] C. M. Lederer and V. S. Shirley, *Table of Isotopes 7th Edition* (Wiley, New York, 1978), Appendix 3.
[10] J. W. Tape, R. Hensler, N. Benczer-Koller, and J. R.

MacDonald, Nucl. Phys. **A195**, 57 (1972).
[11] H. J. Rose and D. M. Brink, Rev. Mod. Phys. **39**, 306 (1967).
[12] E. Sheldon and V. C. Rogers, Comput. Phys. Commun. **6**, 99 (1973).
[13] C. Y. Fu, E. J. Axton, and F. G. Perey, evaluated data base for ^{12}C, National Nuclear Data Center, Brookhaven National Laboratory, Upton, NY (1989); G. Haouat, J. Lachkar, J. Sigaud, Y. Patin, and F. Cocu, Nucl. Science Engr. **65**, 331 (1978).
[14] K. Shibatu, Japan Atomic Energy Research Institute Report JEARI-M-83-221, Tokai, Ibaraki, Japan (1983).
[15] A. E. Blaugrund, Nucl. Phys. **A88**, 501 (1966).
[16] G. A. P. Engelbertink, H. Lindeman, and M. J. N. Jacobs, Nucl. Phys. **A107**, 305 (1968).
[17] N. Benczer-Koller, G. G. Seaman, M. C. Bertin, J. W. Tape, and J. R. MacDonald, Phys. Rev. C **2**, 1037 (1970).
[18] S. Raman, C. H. Malarkey, W. T. Milner, C. W. Nestor, Jr., and P. H. Stelson, At. Data Nucl. Data Tables **36**, 1 (1987).
[19] K. J. Oostrum, R. Hofstadter, G. R. Noldeke, and M. R. Yearian, Phys. Rev. Lett. **16**, 528 (1966).
[20] C. R. Gruhn, T. Y. T. Kuo, C. J. Maggiore, and B. M. Preedom, Phys. Rev. C **6**, 944 (1972).
[21] E. P. Lippincott and A. M. Bernstein, Phys. Rev. **1**, 1170 (1967).
[22] L. G. Multhauf, K. G. Tirsell, S. Raman, J. B. McCrory, Phys. Lett. **57B**, 44 (1975).
[23] J. W. Tape, M. Ulrickson, N. Benczer-Koller, and J. R. MacDonald, Phys. Rev. C **12**, 2125 (1975).
[24] D. E. Alburger, Nucl. Data Sheets **45**, 557 (1985).
[25] R. A. Eisenstein, D. W. Madsen, H. Theissen, L. S. Cardman, and C. K. Bockelman, Phys. Rev. **188**, 1815 (1969).
[26] Y. Fujita, M. Fujiwara, S. Morinobu, T. Yamazaki, T. Itahashi, H. Ikegami, and S. I. Hayakawa, Phys. Rev. C **37**, 45 (1988).
[27] J. E. Wise, J. S. McCarthy, R. Altemus, B. E. Norum, R. R. Whitney, J. Heisenberg, J. Dawson, and O. Schwentker, Phys. Rev. C **31**, 1699 (1985).
[28] E. W. Kleppinger and S. W. Yates, Phys. Rev. C **27**, 2608 (1983).
[29] P. M. Endt, At. Data Nucl. Data Tables **23**, 547 (1979).
[30] R. E. Segel, K. E. Rehm, P. Kienle, J. R. Comfort, and D. W. Miller, Phys. Rev. C **29**, 1703 (1984).
[31] J. W. Tepel, H. M. Hofmann, and H. A. Weidenmuller, Phys. Lett. **49B**, 1 (1974); J. W. Tepel, H. M. Hofmann, and M. Herman, in *Proceedings of the International Conference on Nuclear Cross Sections for Technology, Knoxville, 1979*, Natl. Bur. Stand. Special Pub. No. 594 (U.S. GPO, Washington, D.C., 1980).
[32] J. R. M. Annand, Ph. D. thesis, Ohio University, 1986.
[33] J. Raynal, in *Computing as a Language of Physics* (IAEA, Vienna, 1972); *The Structure of Nuclei* (IAEA, Vienna, 1972), p. 75; Phys. Rev. C **23**, 2571 (1981).
[34] J. S. Hanspal, N. M. Clarke, R. J. Griffiths, O. Karban, and S. Roman, Nucl. Phys. **A462**, 445 (1987).
[35] V. A. Madsen, V. R. Brown, and J. D. Anderson, Phys. Rev. C **12**, 1205 (1975).
[36] A. M. Bernstein, V. R. Brown, and V. A. Madsen, Phys. Letters **103B**, 255 (1981), and references cited therein.
[37] P. W. F. Alons, H. P. Blok, J. F. A. Van Hienen, and J. Blok, Nucl. Phys. **A367**, 41 (1981).
[38] Ch. Lagrange, J. Lachkar, G. Haouat, R. E. Shamu, and M. T. McEllistrem, Nucl. Phys. **A345**, 193 (1980).
[39] G. M. Honoré, W. Tornow, C. R. Howell, R. S. Pedroni, R. C. Byrd, R. L. Walter, and J. P. Delaroche, Phys. Rev. C **33**, 1129 (1986).
[40] E. Gmitrovà, M. Gmitro, and Y. K. Gambhir, Phys. Rev. C **4**, 1239 (1971).
[41] J. B. McGrory, B. H. Wildenthal, and E. C. Halbert, Phys. Rev. C **2**, 186 (1970).
[42] J. B. McGrory and B. H. Wildenthal, Phys. Lett. **103B**, 173 (1981).
[43] P. Federman and S. Pittel, Nucl. Phys. **A155**, 161 (1970).